Stereoelectronic Preferences in Electron Transfer Series of Nickel with Tridentate Ligands Containing Hard–Soft Donor Sets

Thomas L. James, Diane M. Smith, and R. H. Holm*

Department of Chemistry, Harvard University, Cambridge, Massachusetts 02138

Received May 18, 1994[⊗]

A pair of redox-active Ni(II) complexes containing mixed hard–soft donor sets in tridentate ligands have been prepared in order to elucidate ligand properties that promote the stabilization of multiple metal oxidation states within a single complex. The ligands Na(pscoo) (5-(diphenylphosphino)-3-thiapentanoate(1−)) and pspyr (4-(diphenylphosphino)-1-(2-pyridyl)-2-thiabutane) were synthesized in good yield by alkylations of psh (2-(diphenylphosphino)ethanethiol). The corresponding complexes $[Ni(pscoo)_2]$ (**6**) and $[Ni(pspyr)_2(BF_4)_2]$ ($[\mathbf{8}](BF_4)_2$) were readily prepared. Also prepared was $[Ni(pset)_2](BF_4)_2$ ($[\mathbf{4}](BF_4)_2$) by alkylation of $[Ni(ps)_2]$. Compound **6** crystallizes in monoclinic space group $P2_1/c$ with $a = 9.092(2)$ Å, $b = 24.585(7)$ Å, $c = 18.785(3)$ Å, $\beta = 94.11(2)°$, and $Z = 4$. It has a distorted octahedral structure with idealized C_2 symmetry. The compound $[\mathbf{8}](BF_4)_2$ was obtained in triclinic space group $P\bar{1}$ with $a = 10.064(3)$ Å, $b = 10.063(4)$ Å, $c = 11.582(5)$ Å, $\alpha = 96.35(4)°$, $\beta = 106.45(3)°$, $\gamma = 114.54(3)°$, and $Z = 1$. Complex $[\mathbf{8}]^{2+}$ has a centrosymmetric distorted octahedral structure. In methanol, **6** undergoes a reversible oxidation at $E_{1/2} = 0.66$ V (vs SCE) to the Ni(III) species $[\mathbf{6}]^+$, which can be chemically generated by oxidation with $(NH_4)_2[Ce(NO_3)_6]$ at −55 °C, retains the stereochemistry of **6**, and has a $(d_{z^2})^1$ ground state. Complex **6** cannot be reversibly reduced. In contrast, $[\mathbf{8}]^{2+}$ in propylene carbonate exhibits three chemically reversible redox steps, at $E_{1/2} = 0.93$, −0.47, and −1.01 V, which are metal-centered and correspond to the couples Ni(III/II), Ni(II/I), and Ni(I/0), respectively. Complexes $[\mathbf{8}]^{3+}$ and $[\mathbf{8}]^{1+}$ were chemically generated at −55 °C by reaction with $(NH_4)_2[Ce(NO_3)_6]$ and Cp_2Co, respectively; EPR properties confirmed metal-centered redox steps. Characteristics of the electron transfer series based on $[\mathbf{8}]^{2+}$ include close approaches to electrochemical reversibility for Ni(III/II) and Ni(I/0) couples but quasi-reversible behavior for the Ni(II/I) couple. When the electrochemical behavior of the latter couple is compared to that of $[\mathbf{4}]^{2+}$, which is reduced in two essentially reversible steps, a structural change is indicated. The following series (coordination number indicated) is consistent with the experimental results: Ni(III)(6) ⇄ Ni(II)(6) ⇄ Ni(I)(4) ⇄ Ni(0)(4). These results demonstrate that multiple oxidation states of nickel can be stabilized with coordinatively flexible hard–soft ligands that respond to the stereoelectronic preferences of the metal.

Introduction

The ability of transition metals to access multiple oxidation states in a variety of ligand environments is a defining element of coordination chemistry. Several factors, such as coordination number, stereochemistry, and ligand type, contribute to the stabilization of a metal in a given oxidation state. As a metal changes oxidation states, it may exhibit markedly different preferences in its coordination environment, thereby mandating a structural change in its coordination sphere. Structural changes pursuant to electron transfer can range from simple alterations of metal–ligand bond lengths and bond angles to rearrangements, isomerizations, and changes in coordination number.[1] A ligand array that cannot accommodate such changes in the stereoelectronic requirements of the metal places severe constraints on the scope of oxidation states accessible to a given complex.

Our continuing interest in the biological redox chemistry of nickel,[2–4] particularly as related to the stabilization of different oxidation states in NiFe hydrogenases,[5–8] has encouraged us to investigate the problem of stabilizing multiple oxidation states of nickel in a single complex. In the most thoroughly investigated hydrogenase of this type, the enzyme from *Desulfovibrio gigas*, several redox states have been identified when the enzyme is reduced under H_2. The prevailing model for the role of nickel in the enzymatic oxidation of H_2 asserts that only Ni(III) and Ni(II) oxidation states are involved.[9,10] An alternative interpretation suggests that Ni(I)–Ni(III) exist during catalytic turnover;[5,11] the possibility of even a transient Ni(0) intermediate in the reaction cycle has been considered.[12] While we question the feasibility of Ni(0),[13] we recognize the possibility of a transient Ni(I) intermediate, especially in light of recent advances in the stabilization of this oxidation state at mild potentials in a biologically relevant ligand environment.[14,15]

[⊗] Abstract published in *Advance ACS Abstracts,* October 1, 1994.

(1) Geiger, W. E. *Prog. Inorg. Chem.* **1985,** *33,* 275.
(2) Krüger, H.-J.; Holm, R. H. *Inorg. Chem,* **1987,** *26,* 3645.
(3) Krüger, H.-J.; Holm, R. H. *J. Am. Chem. Soc.* **1990,** *112,* 2955.
(4) Krüger, H.-J.; Peng, G.; Holm, R. H. *Inorg. Chem.* **1991,** *30,* 734.
(5) Cammack, R.; Fernandez, V. M.; Schneider, K. In *The Bioinorganic Chemistry of Nickel*; Lancaster, J. R., Jr., Ed.; VCH Publishers, Inc.: New York, 1988; Chapter 8.
(6) Moura, J. J. G.; Teixeira, M.; Moura, I.; LeGall, J. In *The Bioinorganic Chemistry of Nickel*; Lancaster, J. R., Jr., Ed.; VCH Publishers, Inc.: New York, 1988; Chapter 9.
(7) Cammack, R. *Adv. Inorg. Chem.* **1988,** *32,* 297.
(8) Cammack, R. In *Bioinorganic Catalysis*; Reedijk, J., Ed.; Marcel Dekker, Inc.: New York, 1993; Chapter 7.
(9) Teixeira, M.; Moura, I.; Xavier, A. V.; Huynh, B. H.; DerVartanian, D. V.; Peck, H. D., Jr.; LeGall, J.; Moura, J. J. G. *J. Biol. Chem.* **1985,** *260,* 8942.
(10) Teixeira, M.; Moura, I.; Xavier, A. V.; Moura, J. J. G.; LeGall, J.; DerVartanian, D. V.; Peck, H. D., Jr.; Huynh, B. H. *J. Biol. Chem.* **1989,** *264,* 16435.
(11) Cammack, R.; Patil, D. S.; Fernandez, V. M. *Biochem. Soc. Trans.* **1985,** *13,* 572.
(12) van der Zwaan, J. W.; Albracht, S. P. J.; Fontijn, R. D.; Slater, E. C. *FEBS Lett.* **1985,** *179,* 271.
(13) The prediction of a Ni(0) intermediate would not appear to be feasible, given the narrow potential range in which the reduction from Ni(III) to Ni(0) would have to occur and the absence of π-acceptor ligands which conventionally stabilize this oxidation state.

0020-1669/94/1333-4869$04.50/0

Elucidation of the fundamental structural and electronic elements that increase the relative stabilities of several metal-based oxidation states in one complex should be useful in interpreting similar properties of a biological system.

The design of complexes that support several oxidation states requires an understanding of the structural proclivities of nickel. Traditionally, Ni(0) and Ni(I) complexes are stabilized by π-acceptor ligands such as phosphines and arsines. The electron-rich character of these complexes and the stereochemical disposition of d^9 and d^{10} metals dictate a preference for four-coordinate structures, with tetrahedral stereochemistry always observed for the d^{10} case. Nickel(III) complexes generally exhibit tetragonally distorted six-coordinate structures, although planar geometries have been reported as well.[2-4,17-20] Nickel(IV) complexes, by analogy to other d^6 metal centers such as Co(III), favor octahedral coordination. The majority of Ni(III) and Ni(IV) complexes have been synthesized or generated with hard first-row ligands such as amines, fluoride, and oximates,[3,16-18] although a significant corpus of work on the synthesis of high-valent complexes with phosphine and arsine ligation also exists.[21]

Given the differences in optimal coordination environments as dependent on oxidation state, it follows that incorporation of both soft and hard donors into a conformationally flexible multidentate ligand may have advantageous effects. Such a ligand could respond to the changes in the stereoelectronic requirements of the metal so as to facilitate formation of multiple oxidation states within a single complex. This premise has led us to investigate the redox chemistry of nickel complexes containing ligands with mixed hard-soft donor sets derived from the known compounds 2-(diphenylphosphino)ethanethiol (psh, **1**) and 5-(diphenylphosphino)-3-thiapentane (pset, **3**). Functionalization of **1** with hard metal-binding substituents provides a convenient route to the synthesis of multidentate mixed-donor ligands. The species $[Ni(pset)_2]^{2+}$ ($[\mathbf{4}]^{2+}$)[24,25] and other planar phosphino-thioether complexes achieve the Ni(I,0) states at relatively mild potentials.[24,26] The resulting low-valent complexes support oxidative addition reactions of possible biological interest.[25] Modification of other planar Ni(II) complexes with hard pendant donors has been used to stabilize high-valent nickel, but the presence of these substituents usually prevents entrance to the lower oxidation states.[27-29]

We report here our investigation of two new mixed-donor ligands, 5-(diphenylphosphino)-3-thiapentanoate(1-) (pscoo, **5**) and 4-(diphenylphosphino)-1-(2-pyridyl)-2-thiabutane (pspyr, **7**), and their respective Ni(II) complexes $[Ni(pscoo)_2]$ (**6**) and $[Ni(pspyr)_2]^{2+}$ ($[\mathbf{8}]^{2+}$). They are considered in the context of understanding the factors that stabilize various oxidation states of nickel. Pertinent ligands and complexes **1**-**8** and their abbreviations are depicted in Figure 1.

Experimental Section

Preparation of Compounds. Unless noted otherwise, all operations were carried out under a pure dinitrogen atmosphere. Reagents were commercial samples and were not purified further. The compounds psh[22] and $[Ni(ps)_2]$ (**2**)[25,30] were prepared as described. Solvents were dried by standard methods and thoroughly degassed prior to use.

Sodium 5-(Diphenylphosphino)-3-thiapentanoate (5). A solution of Na(psh) prepared from 0.28 g (12.2 mmol) of sodium and 3.0 g (12.2 mmol) of psh in 100 mL of ethanol was added dropwise to a solution of 1.34 g (11.5 mmol) of $ClCH_2CO_2Na$ in 100 mL of ethanol maintained at 0 °C. The reaction mixture was allowed to warm to room temperature with stirring and was stirred for 12 h, during which time a substantial amount of white precipitate formed. The mixture was filtered, and the filtrate was concentrated in vacuo to yield a pasty white solid. This material was washed with a small amount of cold ethanol and then washed extensively with ether. The white powder which resulted was recrystallized by slow addition of ether to a saturated ethanol solution. The solid was collected, washed thoroughly with

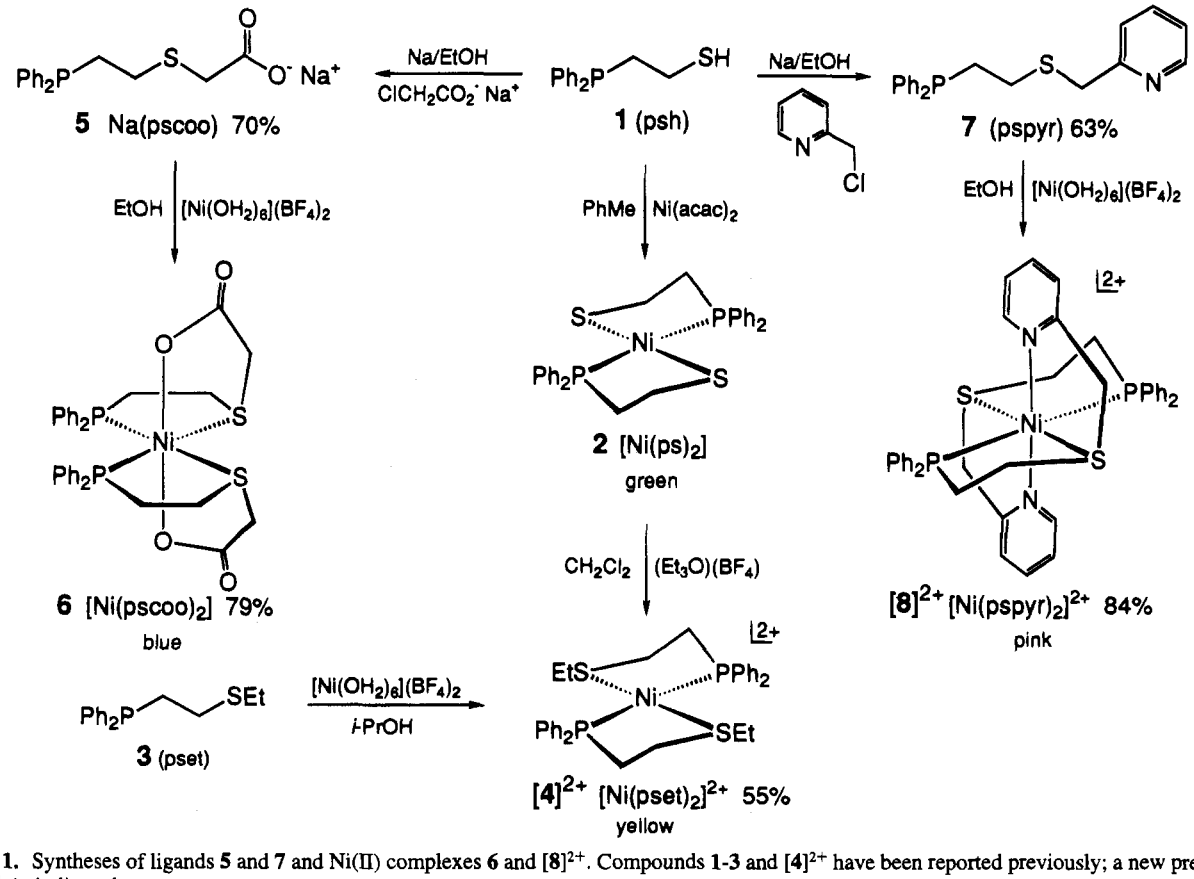

Figure 1. Syntheses of ligands **5** and **7** and Ni(II) complexes **6** and $[\mathbf{8}]^{2+}$. Compounds **1**-**3** and $[\mathbf{4}]^{2+}$ have been reported previously; a new preparation of $[\mathbf{4}]^{2+}$ is indicated.

ether, and dried in vacuo for 48 h to give the product as 2.80 g (70%) of a white solid. FAB-MS (3-nitrobenzyl alcohol): M^+ calcd *m/e* 349.0404, found *m/e* 349.0402. ^1H NMR (MeOD): δ 2.27−2.30 (m, 2), 2.51−2.56 (m, 2), 3.06 (s, 2), 7.22−7.27 (m, 6), 7.33 (t, 4). Anal. Calcd for $C_{16}H_{16}NaO_2PS$: C, 58.88, H, 4.94. Found: C, 58.33; H, 5.07.

4-(Diphenylphosphino)-1-(2-pyridyl)-2-thiabutane (7). A solution of 18.8 mmol of Na(psh) prepared as above was added to a solution of 3.03 g (18.5 mmol) of 2-picolyl chloride (generated from the hydrochloride with NaOEt) in 100 mL of ethanol at 0 °C. The reaction mixture was allowed to warm to room temperature with stirring and was stirred for an additional 10 h, during which time a white precipitate appeared. The mixture was filtered, and the filtrate was taken to dryness in vacuo. To remove residual NaCl, the solid residue was dissolved in toluene, the mixture was filtered, and the filtrate was concentrated in vacuo. The resulting viscous oil was chromatographed in an inert atmosphere box using 230−400 mesh silica gel and 7:3 hexane/ethyl acetate (v/v) eluant. The relevant fractions were combined and concentrated to afford the product as 3.91 g (63%) of a clear viscous oil. EI-MS: M^+ calcd *m/e* 337.1054, found *m/e* 337.1039. ^1H NMR ($CDCl_3$): δ 2.29−2.32 (m, 2), 2.50−2.55 (m, 2), 3.82 (s, 2), 7.13 (dd, 1), 7.27 (d, 1), 7.31−7.33 (m, 6), 7.37−7.40 (m, 4), 7.59 (td, 1), 8.49 (dd, 1). Anal. Calcd for $C_{20}H_{20}NPS$: C, 71.19; H, 5.97; N, 4.15. Found: C, 70.99; H, 5.91; N, 4.05.

Bis(5-(diphenylphosphino)-3-thiapentanoato)nickel(II) (6). A solution of 0.84 g (2.5 mmol) of $[Ni(OH_2)_6](BF_4)_2$ in 30 mL of ethanol was added dropwise to a solution of 1.63 g (5.00 mmol) of Na(pscoo) in 30 mL of ethanol. The royal blue reaction mixture was stirred for 2 h, during which time a light blue precipitate formed. The mixture was reduced in vacuo to about half of the original volume and was filtered. The blue solid was washed several times with 30-mL portions of ether and dried in vacuo for 24 h. The product was obtained as 1.31 g (79%) of blue microcrystalline solid (as the monohydrate). FAB-MS (3-nitrobenzyl alcohol): *m/e* 664 ($M + H^+$). Absorption spectrum (CH_2Cl_2): λ_{max} (ϵ_M) 586 (43), 650 (sh, 23), 924 (22), 1048 nm (sh, 13). Anal. Calcd for $C_{32}H_{34}NiO_5P_2S_2$: C, 56.24; H, 5.01. Found: C, 56.19; H, 4.92. This compound was additionally identified by an X-ray structure determination.

Bis(4-(diphenylphosphino)-1-(2-pyridyl)-2-thiabutane)nickel(II) Tetrafluoroborate ([8](BF$_4$)$_2$). A solution of 1.41 g (4.10 mmol) of $[Ni(OH_2)_6](BF_4)_2$ in 50 mL of ethanol was added dropwise to a solution of 2.80 g (8.30 mmol) of pspyr in 100 mL of ethanol. A pink precipitate immediately formed. The reaction mixture was stirred for 1 h, and the solid was collected by filtration. This material was washed thoroughly with ether, dried in vacuo for 24 h, and recrystallized from acetonitrile/ether. The product was obtained as 3.15 g (84%) of a pink microcrystalline solid. FAB-MS (3-nitrobenzyl alcohol): *m/e* 819 ($M - BF_4$). Absorption spectrum (acetonitrile): λ_{max} (ϵ_M) 524 (42), 548 (sh, 36), 804 nm (38). Anal. Calcd for $C_{40}H_{40}B_2F_8N_2NiP_2S_2$: C, 52.97; H, 4.44; N, 3.09. Found: C, 52.92; H, 4.60; N, 3.06. This compound was additionally identified by an X-ray structure determination.

Table 1. Summary of Crystallographic Data[a]

	$[Ni(pspyr)_2](BF_4)_2$	$[Ni(pscoo)_2]\cdot 3EtOH$
formula	$C_{40}H_{40}B_2F_8N_2NiP_2S_2$	$C_{38}H_{50}NiO_7P_2S_2$
fw	907.1	803.6
crystal system	triclinic	monoclinic
space group	$P\bar{1}$	$P2_1/c$
Z	1	4
a, Å	10.064(3)	9.092(2)
b, Å	10.063(4)	24.585(7)
c, Å	11.582(5)	18.785(3)
α, Å	96.35(4)	
β, Å	106.45(3)	94.11(2)
γ, Å	114.54(3)	
V, Å^3	987.6(7)	4188.1(17)
ϱ_{calc}, g/cm^3	1.52	1.21
μ, mm^{-1}	0.75	0.68
R,[b] R_w,[c] %	5.69, 5.60	6.07, 6.54

[a] Obtained at $T = 233$ K with graphite-monochromatized Mo Kα radiation ($\lambda = 0.710\,69$ Å). [b] $R = \sum||F_o| - |F_c||/\sum|F_o|$. [c] $R_w = \{\sum[w(|F_o| - |F_c|)^2]/\sum[w|F_o|^2]\}^{1/2}$.

Bis(5-(diphenylphosphino)-3-thiapentane)nickel(II) Tetrafluoroborate ([4](BF$_4$)$_2$). This method is an alternative to a previously reported synthesis of this compound, which utilized a sulfur mustard reagent during ligand preparation.[24,25] A solution of 0.35 g (1.82 mmol) of $(Et_3O)(BF_4)$ in 25 mL of dichloromethane at 0 °C was added dropwise to a rapidly stirred solution of 0.46 g (0.84 mmol) of [Ni(ps)$_2$] in 50 mL of dichloromethane at 0 °C. The deep green solution was warmed to room temperature and stirred for 1 h, during which time the color of the reaction mixture changed to orange. The solvent was removed in vacuo and the resulting residue was washed with 3 × 50 mL of ether, giving the crude product as an orange powder which was recrystallized from acetone/ether. The product was obtained as 0.36 g (55%) of an orange crystalline solid. Anal. Calcd for $C_{32}H_{38}B_2F_8NiP_2S_2$: C, 49.22; H, 4.91. Found: C, 49.23; H, 5.23.

Collection and Reduction of X-ray Data. Diffraction-quality crystals of $[Ni(pscoo)_2]\cdot 3EtOH$ (blue plates) and $[Ni(pspyr)_2](BF_4)_2$ (pink elongated plates) were obtained by diffusion of ether into solutions of the compounds in ethanol and nitromethane, respectively. Crystals were mounted in Paratone-N oil and attached to glass fibers. Diffraction data were collected using graphite-monochromatized Mo Kα radiation on a Siemens R3m/v four-circle automated diffractometer equipped with a Siemens LT-2 cryostat operating at 233 K. Unit cell parameters were obtained by least-squares refinement of machine-centered reflections. Intensities of three standard reflections monitored every 97 reflections indicated no significant decay during data collections. Crystallographic data are provided in Table 1. Corrections for Lorentz and polarization effects were applied using the program XDISK of the SHELXTL PLUS program package; empirical absorption corrections were made with the program XEMP. Assignments of space groups from statistics and systematic absences were confirmed by successful structure solutions and refinements.

Solution and Refinement of Structures. Initial structural solutions were obtained by direct methods. All non-hydrogen atoms not located in the initial solutions were found by successive Fourier or difference Fourier maps with intervening cycles of least-squares refinement. All non-hydrogen atoms were described anisotropically in both structures. In the final stages of refinement, hydrogen atoms were placed 0.96 Å from the bonded carbon atoms and were assigned an isotropic temperature factor of 0.08 Å^2. Final difference Fourier maps generally exhibited residual electron density only near solvate molecules in $[Ni(pscoo)_2]\cdot 3EtOH$ and near anions in $[Ni(pspyr)_2](BF_4)_2$, indicating

(14) Mills, D. K.; Reibenspies, J. H.; Darensbourg, M. Y. *Inorg. Chem.* **1990**, *29*, 4364.
(15) (a) Darensbourg, M. Y.; Font, I.; Mills, D. K.; Pala, M.; Reibenspies, J. H. *Inorg. Chem.* **1992**, *31*, 4965. (b) See also: Farmer, P. J.; Reibenspies, J. H.; Lindahl, P. A.; Darensbourg, M. Y. *J. Am. Chem. Soc.* **1993**, *115*, 4665.
(16) Sacconi, L.; Mani, F.; Bencini, A. In *Comprehensive Coordination Chemistry*; Wilkinson, G., Ed.; Pergamon Press: Oxford, U.K., 1987; Vol. 5, pp 1−347.
(17) Nag, K.; Chakravorty, A. *Coord. Chem. Rev.* **1980**, *33*, 87.
(18) Lappin, A. G.; McAuley, A. *Adv. Inorg. Chem.* **1988**, *32*, 241.
(19) Haines, R. I.; McAuley, A. *Coord. Chem. Rev.* **1981**, *39*, 77.
(20) (a) Fox, S.; Wang, Y.; Silver, A.; Millar, M. *J. Am. Chem. Soc.* **1990**, *112*, 3218. This reference reports the generation of a Ni(III)−thiolate complex whose EPR spectrum is consistent with a planar structure. (b) Collins, T. J.; Nichols, T. R.; Uffelman, E. S. *J. Am. Chem. Soc.* **1991**, *113*, 4708.
(21) Levason, W. *Comments Inorg. Chem.* **1990**, *9*, 331.
(22) Chatt, J.; Dilworth, J. R.; Schmutz, J. A.; Zubieta, J. A. *J. Chem. Soc., Dalton Trans.* **1979**, 1595.
(23) Rigo, P.; Bressan, M. *Inorg. Chem.* **1975**, *14*, 1491.
(24) Rigo, P.; Bressan, M.; Basato, M. *Inorg. Chem.* **1979**, *18*, 860.
(25) Hsiao, Y.-M.; Chojnacki, S. S.; Hinton, P.; Reibenspies, J. H.; Darensbourg, M. Y. *Organometallics* **1993**, *12*, 870.
(26) Zotti, G.; Pilloni, G.; Rigo, P.; Martelli, M. *J. Electroanal. Chem. Interfacial Electrochem.* **1981**, *124*, 277.
(27) Kimura, E. *Pure Appl. Chem.* **1986**, *58*, 1461.
(28) Hitaka, Y.; Koike, T.; Kimura, E. *Inorg. Chem.* **1986**, *25*, 402.
(29) Goodman, D.; Tuntulani, T.; Farmer, P. J.; Darensbourg, M. Y.; Reibenspies, J. H. *Angew. Chem., Int. Ed. Engl.* **1993**, *32*, 116.
(30) Pfeiffer, E.; Pasquier, M. L.; Marty, W. *Helv. Chim. Acta* **1984**, *67*, 654.

Table 2. Positional Parameters ($\times 10^4$) for the Non-Hydrogen Atoms in $[Ni(pscoo)_2]\cdot 3EtOH$

atom	x/a	y/b	z/c
Ni(1)	4134(1)	7173(1)	6104(1)
S(1)	2566(3)	6405(1)	5704(2)
S(2)	5242(3)	7143(1)	4943(1)
P(1)	2838(3)	7163(1)	7163(1)
P(2)	5779(3)	7915(1)	6394(1)
O(1)	2404(7)	7614(3)	5672(4)
O(2)	304(8)	7681(4)	5007(4)
O(3)	5805(8)	6652(3)	6386(4)
O(4)	7772(8)	6154(4)	6133(5)
O(5)	31(10)	1302(4)	4486(7)
O(6)	1418(15)	945(6)	7439(6)
O(7)	4561(50)	31(16)	1866(24)
C(1)	1358(11)	7406(5)	5270(6)
C(2)	1324(12)	6805(5)	5122(6)
C(3)	1469(12)	6299(5)	6466(6)
C(4)	1097(11)	6816(5)	6860(6)
C(5)	3415(12)	6776(4)	7957(6)
C(6)	4657(12)	6451(5)	7944(6)
C(7)	5086(14)	6143(5)	8540(6)
C(8)	4310(15)	6155(5)	9142(7)
C(9)	3098(13)	6488(5)	9157(6)
C(10)	2653(12)	6799(5)	8570(6)
C(11)	2320(11)	7822(5)	7509(6)
C(12)	1158(12)	8120(6)	7193(7)
C(13)	882(16)	8629(6)	7425(8)
C(14)	1779(18)	8854(6)	7967(8)
C(15)	2934(17)	8569(6)	8288(8)
C(16)	3182(13)	8068(5)	8054(6)
C(17)	6687(13)	6455(5)	5960(7)
C(18)	6350(13)	6559(5)	5160(6)
C(19)	6578(13)	7697(5)	5043(6)
C(20)	7231(11)	7780(5)	5790(6)
C(21)	6797(11)	7943(5)	7268(5)
C(22)	7503(11)	7464(5)	7521(6)
C(23)	8302(13)	7453(6)	8173(6)
C(24)	8414(12)	7936(7)	8562(6)
C(25)	7683(15)	8389(6)	8335(7)
C(26)	6879(13)	8399(5)	7687(6)
C(27)	5267(11)	8611(4)	6209(5)
C(28)	6305(14)	9022(5)	6131(6)
C(29)	5870(14)	9552(5)	5986(7)
C(30)	4389(15)	9688(6)	5952(7)
C(31)	3359(14)	9275(6)	6034(7)
C(32)	3753(11)	8740(5)	6157(6)
C(51)	385(31)	767(17)	4996(18)
C(52)	1165(29)	1031(11)	5408(13)
C(61)	1052(27)	385(8)	7399(12)
C(62)	−483(24)	232(10)	7024(13)
C(71)	4888(60)	−47(17)	1193(37)
C(72)	4675(55)	350(14)	630(18)

possible disorder which was not refined further. Final R values are set out in Table 1 and positional parameters in Tables 2 and 3.[31]

Other Physical Measurements. FAB and EI mass spectra were collected using either a JEOL AX505H or a JEOL SX102A mass spectrometer. Absorption spectra were recorded on Varian 2390 and Perkin-Elmer Lambda 4C spectrophotometers. For Nujol mull spectra, background corrections were made with calcium carbonate. Solid state magnetic susceptibilities were measured on a Johnson-Mathey magnetic susceptibility balance. NMR spectra were obtained on a Bruker AM-300 NMR spectrometer. Solution susceptibilities were measured by the standard NMR method.[32] EPR spectra were taken on a Bruker ESP 300-E spectrometer operating at X-band frequencies. All spectra were recorded at 120 K using a Bruker ER 412VT-E10 liquid nitrogen variable-temperature apparatus. A standard calibration curve for integration of Ni-based samples was made using varying concentrations of $CuSO_4$ in 1:1 glycerol/water as the external standard. Integrated spectra were corrected for transition probability differences between

(31) See paragraph at the end of this article concerning supplementary material available.

(32) Live, D. H.; Chan, S. I. *Anal. Chem.* **1970**, *42*, 791.

Table 3. Positional Parameters ($\times 10^4$) for the Non-Hydrogen Atoms in $[Ni(pspyr)_2](BF_4)_2$

atom	x/a	y/b	z/c
Ni(1)	0	0	0
N(1)	755(8)	561(7)	1958(6)
P(1)	−2006(3)	−2624(3)	−142(2)
S(1)	−1963(3)	716(3)	182(2)
C(1)	1723(10)	137(10)	2689(7)
C(2)	2130(11)	398(11)	3952(8)
C(3)	1481(12)	1099(12)	4504(9)
C(4)	488(11)	1557(12)	3803(8)
C(5)	138(10)	1272(10)	2532(7)
C(6)	−799(10)	1909(10)	1760(7)
C(7)	−3392(10)	−877(9)	474(8)
C(8)	−3756(9)	−2386(10)	−384(8)
C(9)	−1675(10)	−3270(10)	1275(7)
C(10)	−335(10)	−3438(10)	1702(8)
C(11)	−29(11)	−3999(11)	2725(9)
C(12)	−1082(13)	−4349(11)	3347(9)
C(13)	−2395(11)	−4183(11)	2945(9)
C(14)	−2705(10)	−3635(10)	1905(8)
C(15)	−2810(9)	−4368(9)	−1383(7)
C(16)	−2978(10)	−5742(10)	−1122(8)
C(17)	−3624(10)	−7026(10)	−2088(8)
C(18)	−4092(10)	−6964(11)	−3329(8)
C(19)	−3910(10)	−5606(11)	−3570(8)
C(20)	−3304(10)	−4334(11)	−2620(8)
F(1)	7671(7)	2371(9)	4067(6)
F(2)	5353(9)	504(8)	3853(7)
F(3)	5534(8)	2673(7)	3551(6)
F(4)	5841(9)	1219(9)	2168(5)
B(1)	6109(14)	1648(13)	3401(10)

standard and sample.[33] Electrochemical experiments were done in an inert atmosphere box using an EG&G Model 263 Potentiostat. Low-temperature experiments were conducted by immersing an electrochemical cell, equipped with ground-glass joints for anaerobic work, in an acetone/dry ice bath. For cyclic voltammetric experiments, 1−2 mM solutions of complexes containing 0.2 M $(Bu_4N)(PF_6)$ or $(Bu_4N)(ClO_4)$ supporting electrolyte were used. Platinum disk, Pt foil, and glassy carbon electrodes were employed as working electrodes. All potentials were determined vs a SCE reference electrode. Internal resistances of solutions were measured, and the appropriate positive feedback corrections were applied.

Results and Discussion

Preparation and Properties of Ni(II) Complexes. The tridentate ligands Na(pscoo) and pspyr and their complexes were prepared according to the procedures in Figure 1. The following complexes are of principal interest in this work:

$[Ni(ps)_2]$	**2**
$[Ni(pset)_2]^{2+}$	$[\mathbf{4}]^{2+}$
$[Ni(pscoo)_2]$	**6**
$[Ni(pspyr)_2]^{2+}$	$[\mathbf{8}]^{2+}$

Of these, **2**[25,30] and $[\mathbf{4}]^{2+}$,[24,25] both of which are planar,[25] have been previously reported. In this work, $[\mathbf{4}]^{2+}$ was obtained from **2** in 55% yield by an alkylation reaction. After recrystallization from ethanol/ether, **6** was obtained as blue plates that are soluble in polar organic solvents such as dichloromethane, acetonitrile, methanol, and propylene carbonate. The compound $[\mathbf{8}](BF_4)_2$ was isolated as dark pink prisms upon recrystallization from acetonitrile/ether; good solubility was observed only in acetonitrile, nitromethane, and propylene carbonate. These two complexes are air-stable for several hours in solution and are indefinitely stable in the solid state.

(33) Aasa, R.; Vänngård, T. *J. Magn. Reson.* **1975**, 308.

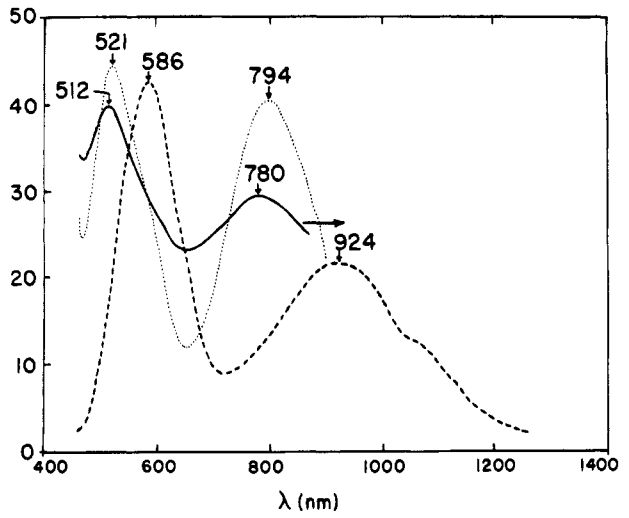

Figure 2. Absorption spectra of $[Ni(pscoo)_2]$ in dichloromethane (- - -) and of $[Ni(pspyr)_2](BF_4)_2$ in propylene carbonate (•••) and a Nujol mull (—).

Spectral and magnetic data indicate that complexes **6** and $[\mathbf{8}]^{2+}$ are octahedral in the solid and solution states. Magnetic moments at *ca.* 300 K are 3.12 μ_B (solid) and 3.14 μ_B (chloroform) for **6** and 3.10 μ_B (solid, nitromethane) for $[\mathbf{8}]^{2+}$. The solution absorption spectra of these complexes in Figure 2 reveal well-resolved bands corresponding to the transitions $^3A_{2g} \rightarrow {}^3T_{2g}$ (ν_1), $^3T_{1g}$ (ν_2) of octahedral Ni(II). The ν_3 bands at higher energies are obscured by charge transfer absorption in both cases. Shoulders on the low-energy sides of these bands indicate splittings of bands of octahedral parentage. In several different solvents, the spectra of **6** and $[\mathbf{8}]^{2+}$ remain essentially the same, exhibiting only slight variations in positions and intensities of the d−d bands. More specifically, the d−d region of $[\mathbf{8}]^{2+}$ remains constant in nitromethane, acetonitrile, and propylene carbonate, indicating that an octahedral structure is maintained in solvents of different donor numbers.[34] Furthermore, the spectrum of $[\mathbf{8}](BF_4)_2$ in a Nujol mull (Figure 2) is practically the same as the solution spectra, with the ν_1 and ν_2 bands slightly blue-shifted by 14 and 9 nm, respectively. The ^1H NMR spectra (not shown) of **6** in chloroform and $[\mathbf{8}]^{2+}$ in nitromethane are both consistent with a single paramagnetic species.

Structures. The crystallographically determined structures of complexes **6** and $[\mathbf{8}]^{2+}$ are presented in Figures 3 and 4, respectively. Selected metric parameters are contained in Tables 4 and 5. Both complexes have facially coordinated ligands and exhibit distorted octahedral stereochemistry. Complex $[\mathbf{8}]^{2+}$ has an imposed symmetry center.

Complex **6** approaches idealized C_2 symmetry with the pseudosymmetry axis bisecting the angles P(1)−Ni−P(2) and S(1)−Ni−S(2). The P_2S_2 portion of the coordination unit defines a plane in which the phosphorus and sulfur atoms are in mutually cis positions; coordination is completed by two carboxylate oxygen atoms in trans positions. While this geometry seems unfavorable on steric grounds, forcing the bulky diphenylphosphino groups close to each other, it accommodates the electronic preference dictated by the trans influence, placing the weaker thioether donors trans to the phosphines. In contrast, $[\mathbf{8}]^{2+}$ adopts an all-trans structure. The steric congestion imposed by coordination of the pyridyl groups apparently overrides the electronic tendency favoring a cis NiP_2S_2 arrangement.

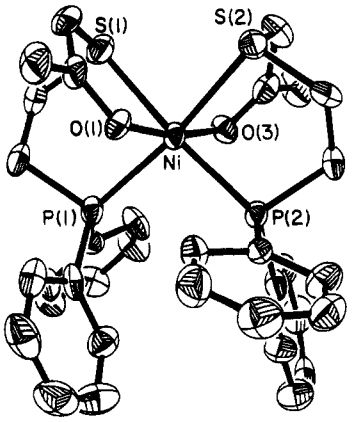

Figure 3. Structure of $[Ni(pscoo)_2]$ showing 50% probability ellipsoids and the atom labeling scheme.

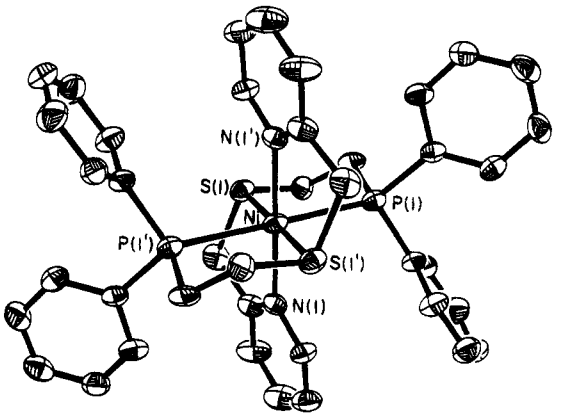

Figure 4. Structure of $[Ni(pspyr)_2]^{2+}$ as the BF_4^- salt, showing 50% probability ellipsoids and the atom-labeling scheme. Primed and unprimed atoms are related by an inversion center.

Table 4. Selected Interatomic Distances (Å) and Angles (deg) for $[Ni(pscoo)_2]\cdot 3EtOH$

Ni(1)−S(1)	2.450(3)	Ni(1)−P(2)	2.397(3)
Ni(1)−S(2)	2.468(3)	Ni(1)−O(1)	2.031(7)
Ni(1)−P(1)	2.384(3)	Ni(1)−O(3)	2.028(7)
S(1)−Ni(1)−S(2)	88.4(1)	S(2)−Ni(1)−O(3)	82.3(2)
S(1)−Ni(1)−P(1)	86.3(1)	P(1)−Ni(1)−P(2)	99.0(1)
S(1)−Ni(1)−P(2)	174.7(1)	P(1)−Ni(1)−O(1)	85.7(2)
S(1)−Ni(1)−O(1)	82.6(2)	P(1)−Ni(1)−O(3)	100.4(2)
S(1)−Ni(1)−O(3)	90.1(2)	P(2)−Ni(1)−O(1)	97.9(2)
S(2)−Ni(1)−P(1)	174.0(1)	P(2)−Ni(1)−O(3)	88.7(2)
S(2)−Ni(1)−P(2)	86.3(1)	O(1)−Ni(1)−O(3)	170.2(3)
S(2)−Ni(1)−O(1)	90.9(2)		

Table 5. Selected Interatomic Distances (Å) and Angles (deg) for $[Ni(pspyr)_2](BF_4)_2$

Ni(1)−N(1)	2.103(6)	Ni(1)−S(1)	2.419(3)
Ni(1)−P(1)	2.523(2)		
N(1)−Ni(1)−N(1')	180.0(1)	P(1)−Ni(1)−P(1')	180.0(1)
N(1)−Ni(1)−S(1)	82.7(2)	S(1)−Ni(1)−N(1')	97.3(2)
N(1)−Ni(1)−S(1')	97.3(2)	S(1)−Ni(1)−S(1')	180.0(1)
N(1)−Ni(1)−P(1)	90.9(2)	S(1)−Ni(1)−P(1')	95.6(1)
N(1)−Ni(1)−P(1')	89.1(2)	N(1')−Ni(1)−S(1')	82.7(2)
P(1)−Ni(1)−N(1')	89.1(2)	N(1')−Ni(1)−P(1')	90.9(2)
P(1)−Ni(1)−S(1)	84.4(1)	P(1')−Ni(1)−S(1')	84.4(1)
P(1)−Ni(1)−S(1')	95.6(1)		

For the most part, **6** and $[\mathbf{8}]^{2+}$ are dimensionally unexceptional; metal−ligand distances are near mean values for other paramagnetic Ni(II) complexes.[35] As expected, Ni−P and Ni−S

(34) Gutmann, V. *The Donor-Acceptor Approach to Molecular Interactions*; Plenum Press: New York, 1978; Chapter 2.

(35) Orpen, A. G.; Brammer, F. H.; Allen, O. K.; Watson, R. T. *J. Chem. Soc., Dalton Trans.* **1989**, Suppl. S1.

Table 6. Electrochemical and EPR Data

complex	solvent	v, mV/s	E, V,[a] followed by ΔE_p, mV Ni(III/II)	Ni(II/I)	Ni(I/0)	g, a values
$[Ni(pscoo)_2]^{0/+}$	MeOH[b]		0.66	c	c	Ni(III) $g_\perp = 2.16$, $g_\parallel = 2.02$, $a_\parallel^P = 8.0$ G
		20	90			
		50	110			
$[Ni(pspyr)_2]^{3+/2+/+/0}$	PC[d]		0.93	−0.47	−1.01	Ni(III) $g_1 = 2.18$, $g_2 = 2.08$, $g_3 = 2.02$, $a_3^N = 16$ G
		20	70	180	70	
		50	70	200	80	
		100	90	220	90	Ni(I) $g_1 = 2.18$, $a_1^P = 60$ G; $g_2 = 2.14$, $a_2^P \sim 60$ G; $g_3 = 2.01$, $a_3^P = 40$ G
		200	110	250	110	
		300	130	280	130	
$[Ni(pset)_2]^{2+/+/0}$	PC[d]		c	−0.27	−0.88	e
		20		70	70	
		50		90	80	
		100		100	80	
		200		130	90	
		300		160	110	

[a] Vs SCE; Pt disk working electrode. [b] 0.2 M $(Bu_4N)(PF_6)$. [c] Irreversible. [d] Propylene carbonate; 0.2 M $(Bu_4N)(ClO_4)$. [e] Not measured.

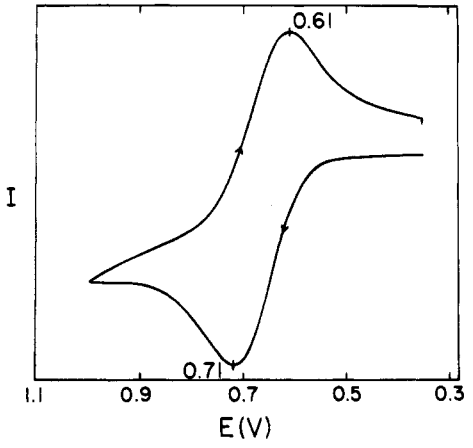

Figure 5. Cyclic voltammogram (50 mV/s) of $[Ni(pscoo)_2]$ in methanol solution at 25 °C, demonstrating a chemically reversible oxidation at $E_{1/2} = 0.66$ V. Peak potentials vs SCE are indicated.

bond lengths are substantially longer (by 0.2−0.3 Å) than those of diamagnetic **2** and $[4]^{2+}$, whose NiP_2S_2 units are trans.[25] The mean Ni−S distance of 2.459 Å in **6** is somewhat longer than typical values for Ni(II)−thioether binding (*ca.* 2.42 Å),[35,36] an effect apparently due to the trans influence of the phosphine group. The most striking feature of $[8]^{2+}$ is the Ni−P bond length 2.523(2) Å, which is the longest such bonded distance reported. Again, a combination of steric crowding of the pyridyl and diphenylphosphino groups and the mutual trans influence of phosphines contribute to the bond lengthening. With the establishment of six-coordinate structures of **6** and $[8]^{2+}$ in the solid state and in solution, we next turn to the matter of electron transfer reactions and associated structures with emphasis on $[8]^{2+}$.

Electron Transfer Behavior. Electrochemical potentials and EPR data for complexes chemically generated *in situ* are collected in Table 6.

(a) Ni(pscoo)$_2$. The cyclic voltammogram of **6** in methanol solution, shown in Figure 5, reveals a one-electron oxidation with $E_{1/2} = 0.66$ V. The peak-to-peak separation $\Delta E_p = 90$ mV at scan rate $v = 20$ mV/s and 110 mV at 50 mV/s. These and other observations indicate that this step is electrochemically quasi-reversible and chemically reversible ($i_{pa}/i_{pc} \approx 1$).[37] The metal-centered nature of the oxidation of **6** was confirmed by the chemical generation of the Ni(III) complex $[6]^+ = [Ni(pscoo)_2]^+$. Reaction of the Ni(II) complex with 1.2 equiv of $(NH_4)_2[Ce(NO_3)_6]$[38] in methanol solution at −55 °C afforded an orange solution that is stable for hours at low temperature but decomposes over a 15-min period when warmed to room temperature. The EPR spectrum of $[6]^+$, shown in Figure 6, is axial with $g_\perp = 2.16$ and $g_\parallel = 2.02$; spectral integration indicated that 83% of nickel is present in the oxidized form. A cyclic voltammogram of the oxidized solution at −20 °C exhibited the same redox couple as that of the initial solution. Hyperfine splitting by two equivalent ^{31}P nuclei is resolved in the $g_\parallel$ feature but is small, with $a_\parallel^P = 8.0$ G. The large anisotropy in g, $g_\perp > g_\parallel \approx 2$, and the small $a_\parallel^P$ value (vide infra) are consistent with a low-spin, effectively tetragonal Ni(III) species with electron configuration ... $(d_{z^2})^1$.[18,39,40] Further, the lack of rhombicity implies that the *cis*-NiP_2S_2 arrangement of **6** is retained in the Ni(III) product.[41]

While the foregoing results demonstrate that oxidation of **6** yields a Ni(III) complex of overall stereochemistry the same as that of the Ni(II) precursor, electrochemical reduction led only to an irreversible process with $E_p \lesssim -1.0$ V. Consequently, attention is directed to the related octahedral complex $[8]^{2+}$.

(b) Ni(pspyr)$_2$]$^{2+}$. The cyclic voltammogram of $[8]^{2+}$ in propylene carbonate, shown in Figure 7, displays three electron transfer processes, one oxidative with $E_{1/2} = 0.93$ V and two reductive with $E_{1/2} = -0.47$ and −1.01 V. All are electrochemically quasi-reversible and chemically reversible. Optimal

(36) (a) Setzer, W. N.; Ogle, C. A.; Wilson, G. S.; Glass, R. S. *Inorg. Chem.* **1983**, *22*, 266. (b) Hintza, E. J.; Hartman, J. R.; Cooper, S. R. *J. Am. Chem. Soc.* **1983**, *105*, 3738. (c) Fortier, D. G.; McAuley, A. *Inorg. Chem.* **1989**, *28*, 655. (d) Boeyens, J. C. A.; Dobson, S. J.; Hancock, R. D. J. *Inorg. Chem.* **1985**, *24*, 3073.

(37) Brown, E. R.; Large, R. F. In *Electrochemical Methods*; Weissberger, A., Rossiter, B., Eds.; *Physical Methods in Chemistry*, Part IIA; Wiley-Interscience: New York, 1971; Chapter VI.

(38) Potentials in propylene carbonate at −20 °C: $(NH_4)_2[Ce(NO_3)_6]$, $E_{1/2} = 1.00$ V; Cp_2Co, $E_{1/2} = -1.06$ V. Reduction of $(NH_4)_2[Ce(NO_3)_6]$ in methanol occurs beyond the anodic solvent cutoff (*ca.* 1.3 V) and could not be measured.

(39) Maki, A. H.; Edelstein, N.; Davison, A.; Holm, R. H. *J. Am. Chem. Soc.* **1964**, *86*, 4580.

(40) Lappin, A. G.; Murray, C. K.; Margerum, D. W. *Inorg. Chem.* **1978**, *17*, 1630.

(41) As seen in Figure 6, the presence of a minor rhombic species with $g \approx 2.20$, 2.09, 2.03 distorts the triplet in the $g_\parallel$ feature of the major signal. The intensity of the minority spectrum is proportional to the amount of unoxidized Ni(II) as determined from concentrations and spectral integrations; we think it likely that the impurity is a mixed-valent species.

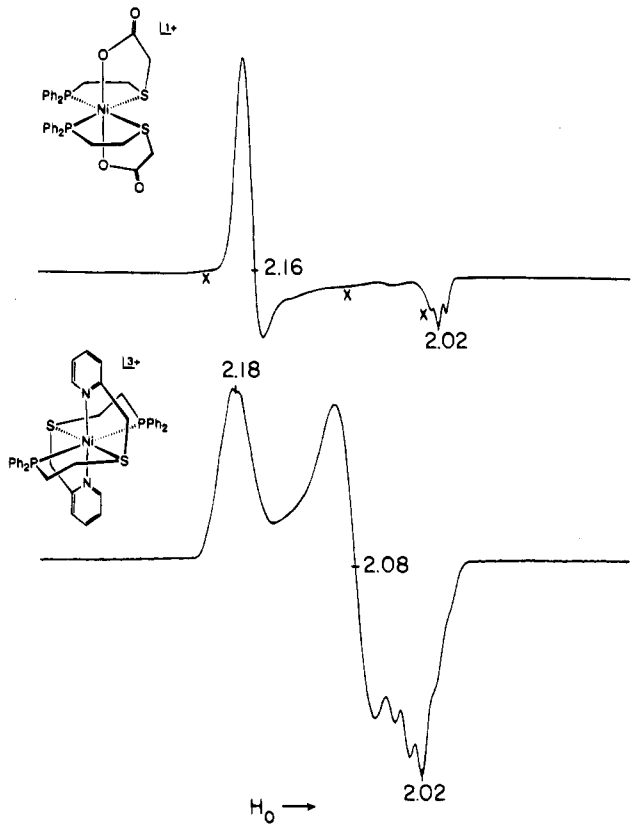

Figure 6. X-Band EPR spectra of $[Ni(pscoo)_2]^+$ in methanol and $[Ni(pspyr)_2]^{3+}$ in propylene carbonate at 120 K. Signals marked with an "x" are those of impurities.[41] Both complexes were generated *in situ* by oxidation of their Ni(II) precursors with $(NH_4)_2[Ce(NO_3)_6]$.

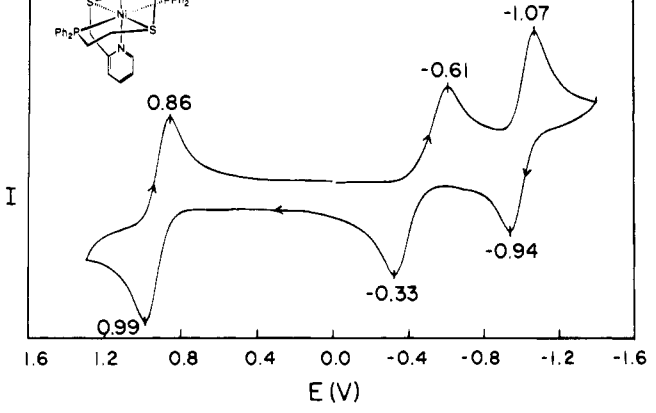

Figure 7. Cyclic voltammogram (300 mV/s) of $[Ni(pspyr)_2](BF_4)_2$ in propylene carbonate solution at 25 °C, demonstrating chemically reversible oxidative and reductive processes at $E_{1/2} = 0.93$, −0.47, and −1.01 V. Peak potentials vs SCE are indicated.

peak resolution and chemical reversibility were obtained using a scan rate of 300 mV/s in propylene carbonate solution.[42] Higher scan rates decreased the resolution between the reductive steps, while at lower scan rates decomposition of the product of the second reduction step introduced several obscuring features into the voltammogram below *ca.* −0.5 V. In order to determine if these processes are metal-centered, oxidation and

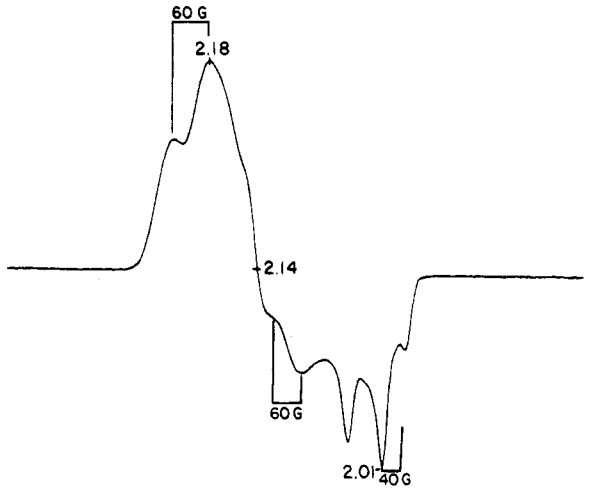

Figure 8. X-Band EPR spectrum of $[Ni(pspyr)_2]^{1+}$ in propylene carbonate at 120 K. ^{31}P hyperfine splittings in three overlapping triplets are indicated. The complex was generated *in situ* by reduction of its Ni(II) precursor with Cp_2Co.

reduction products were generated *in situ* by chemical means in propylene carbonate solution.

Oxidation of $[\mathbf{8}]^{2+}$ with 1.2 equiv of $(NH_4)_2[Ce(NO_3)_6]$[38] at −55 °C produced a deep purple solution that is stable at low temperatures for hours but decomposes within 5 min upon warming above −20 °C. The EPR spectrum of the oxidation product is shown in Figure 6. The spectrum is rhombic, with principal g values $g_1 = 2.18$, $g_2 = 2.08$, and $g_3 = 2.02$ and clearly arises from low-spin Ni(III) in the complex $[\mathbf{8}]^{3+} = [Ni(pspyr)_2]^{3+}$. Spin quantitation indicated 80% conversion to Ni(III). Hyperfine coupling to ^{14}N is resolved in a quintet pattern on the $g_3 = g_{zz} = 2.02$ line with $a_{zz}^N = 16.0$ G. No hyperfine structure from coupling to ^{31}P is resolvable. The rhombicity of the spectrum requires that all molecular axes be unique, indicating that the centrosymmetric structure with trans ligand orientations is preserved upon oxidation to form $[\mathbf{8}]^{3+}$. A distorted octahedral structure with the unpaired electron placed in a d_{z^2} orbital along the N−Ni−N axis is consistent with the EPR results.

Reduction of $[\mathbf{8}]^{2+}$ with 1.2 equiv of Cp_2Co[38] at −55 °C affords an air-sensitive golden solution that is stable at low temperatures but decomposes rapidly upon warming to room temperature. The EPR spectrum of the reduction product, presented in Figure 8, is rhombic with the apparent g values $g_1 = 2.18$, $g_2 = 2.14$, and $g_3 = 2.01$; each line is split into a triplet from coupling to two ^{31}P nuclei (Table 6). Spin quantitation indicated that the spectrum corresponds to an 86% reduction to the complex $[\mathbf{8}]^+ = [Ni(pspyr)_2]^+$. No ^{14}N hyperfine coupling could be detected; while this does not rule out coordination of the pyridyl groups, the absence of coupling is consistent with a four-coordinate structure. The EPR data suggest a NiP_2S_2 coordination unit. Significant hyperfine splitting of each rhombic component further suggests that the foregoing unit is not planar. While the reduction reaction has without doubt afforded a Ni(I) product,[43] we are unable to specify the ground state without knowledge of the molecular orientation of the **g** tensor.

(42) Decidedly inferior voltammograms, in terms of observing three processes and/or approaching chemical reversibility, were obtained in dichloromethane (which reacts with reduced nickel species), nitromethane, and acetonitrile. The limited solubility of $[\mathbf{8}](BF_4)_2$ prevented further examination of solvent dependence.

(43) The identity of this product is strongly supported by the obvious similarity of its EPR spectrum to that of a structurally characterized Ni(I) complex with distorted square pyramidal NiP_2S_2N ligation ($g_1 = 2.25$, $g_2 = 2.18$, $g_3 = 2.05$, $a_1 = 44$ G, $a_2 = 41$ G, $a_3 = 45$ G): James, T. L.; Muetterties, M. C.; Holm, R. H. Results to be published. In this molecule, as opposed to $[\mathbf{8}]^+$, a five-coordinate structure is stabilized by the pentadentate ligand structure.

Oxidized and reduced solutions containing at least 80% of the redox product were examined by cyclic voltammetry at −30 °C (oxidized) and −20 °C (reduced). With allowance for temperature difference and overlap with features of the redox reagents, the nickel-based steps matched those of $[\mathbf{8}]^{2+}$ (Figure 7). Thus, the chemically generated EPR-active species are identical with those produced electrochemically.

A conspicuous feature of voltammetry of $[\mathbf{8}]^{2+}$ is the large peak-to-peak separation $\Delta E_p = 280$ mV for the Ni(II/I) couple ($E_{1/2} = -0.47$ V) in Figure 7; this voltammogram was recorded using a Pt disk working electrode and 0.2 M $(Bu_4N)(ClO_4)$ supporting electrolyte (E1). Values of ΔE_p for the other two couples (130 mV) are not unusual for electrochemically quasi-reversible reactions of metal complexes in nonaqueous solvents. To ascertain whether the effect is intrinsic to this couple or is due to the extrinsic factors of electrode and supporting electrolyte, additional experiments at constant scan rate (v = 300 mV/s) were performed. The nature of the electrode can influence adsorption and otherwise bias the rate of heterogeneous electron transfer because the potential of the double layer is responsive to electrode composition.[44] Further, it has been suggested that ion-pairing effects associated with the electrolyte can influence electron transfer kinetics, with those electrolytes forming tighter ion pairs with the electroactive complex promoting faster electron transfer.[45a]

For the Ni(II/I) couple at a Pt electrode, $\Delta E_p = 290$ mV in the presence of 0.2 M $(Bu_4N)(PF_6)$ (E2). At a glassy carbon electrode, $\Delta E_p = 350$ mV in the presence of E2 and 400 mV in a solution of E1. The ΔE_p value for the Ni(I/0) couple is 130 mV under all conditions tested, while the value for the Ni(III/II) couple varied over the range 120−180 mV. From these observations we conclude that the values $\Delta E_p = 280-400$ mV for the Ni(II/I) couple reflect an intrinsic property leading to relatively slow heterogeneous electron transfer rates.

Electron Transfer Scheme. An important difference between the Ni(III/II) and the Ni(I/0) couples and the Ni(II/I) couple based on $[\mathbf{8}]^{2+}$ is evident from the ΔE_p data in Table 6. The first two couples approach electrochemically reversible behavior at low scan rates ($\Delta E_p \approx 60$ mV), whereas decidedly larger ΔE_p values are observed for the Ni(II/I) couple at all scan rates. The relatively large peak-to-peak separation in the Ni(II/I) couple is consistent with a rate-limiting structural change in this electron transfer step. In the limiting case of large structural alterations, the activation barrier may be sufficiently high to slow the heterogeneous electron transfer rates, resulting in electrochemically quasi-reversible or irreversible behavior.[1]

Such behavior may be understood in terms of the four-component (ECEC) scheme proposed by Geiger[1] and summarized as

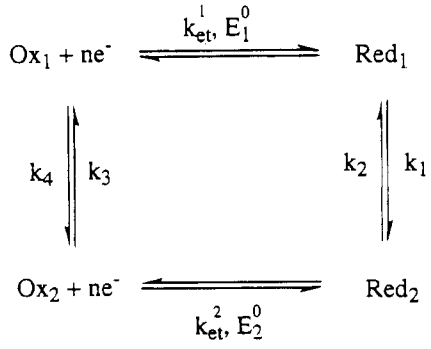

According to this model, the overall electron transfer $Ox_1 + e^- \rightleftarrows Red_2$ can be considered to occur in two steps. Initial electron transfer to Ox_1 at potential E°_1 with heterogeneous rate constant k^1_{et} results in formation of intermediate Red_1, whose structure closely resembles that of the reactant. Red_1 then undergoes isomerization with rate constant k_1 to form product Red_2. The reverse of this two-step process holds for the oxidation of Red_2, which proceeds through intermediate Ox_2 followed by isomerization to Ox_1. When k_1 is small, intermediate Red_1 should be sufficiently long-lived to be detectable by standard voltammetric techniques. If k_1 is large, however, the electron transfer event and the chemical reaction can have comparable rates, and the detection of Red_1 is prohibited. In this limiting case, fast distortions of a reversible nature should lead to quasi-reversible charge transfer kinetics.

We propose that the electrochemical behavior of the Ni(II/I) couple of $[\mathbf{8}]^{2+}$ can be described by a rate-limiting structural change which can be understood in terms of the fast limit of the ECEC mechanism. Given the preference which low-valent nickel displays for coordination numbers below 6 and soft donor sets, the most likely structural change to occur upon electrochemical reduction of the Ni(II) complex is decoordination of the two pendant pyridyl donors, yielding a four-coordinate Ni(I) complex with a soft P_2S_2 donor set. In this regard, note that the related complex $[\mathbf{4}]^{2+}$, which lacks pendant nitrogen coordination, undergoes two chemically reversible reductions in propylene carbonate with potentials roughly comparable to those of $[\mathbf{8}]^{2+/+/0}$ (Table 6). Both couples approach reversible behavior as the scan rate is decreased from 300 to 20 mV/s. Also, the approach to reversibility of the Ni(I/0) couple compares very favorably to the corresponding behavior of the $[\mathbf{8}]^{+/0}$ couple.

Under the ECEC model, an initial six-coordinate Ni(I) compound should form upon electron transfer, followed by isomerization to the four-coordinate species. Detection of the six-coordinate intermediate is dependent upon the magnitude of the rate constant for isomerization to the four-coordinate entity. Cyclic voltammograms run with high scan rates (*ca.* 500 mV/s−1 V/s) or at low temperature (−30 °C) show no resolution of a peak attributable to a six-coordinate intermediate. Quasi-reversible behavior is observed under all conditions employed. In a related case, Geiger and co-workers[46] have encountered similar difficulty in intermediate detection by cyclic voltammetry in the reduction of (1,5-COT)CoCp to [(1,3-COT)CoCp]$^-$ in which the cyclooctatetraene undergoes a shift in coordination mode. In this case the rate of isomerization was determined by fast Fourier transform faradaic admittance measurements to be $(2 + 1) \times 10^{-3}$ s.$^{-1}$ The nature of the structural rearrangement proposed for $[\mathbf{8}]^{1+}$ suggests that the rate constant for this process could easily fall into a similar regime and, therefore, suggests a reason for the difficulty in the detection of a redox intermediate by cyclic voltammetry.

The four-membered electron transfer series based on $[\mathbf{8}]^{2+}$ is depicted in Figure 9 with established and proposed structures, which have crystallographic precedent.[16,47-49] EPR data demonstrate coordination of both pendant pyridyl ligands in $[\mathbf{8}]^{3+}$

(44) Bard, A. J.; Faulkner, L. R. *Electrochemical Methods*; Wiley: New York, 1980; Chapter 12.
(45) (a) Downard, A. J.; Hanton, L. R.; McMorran, D. A.; Paul, R. L. *Inorg. Chem.* **1993**, *32*, 6028. (b) Downard, A. J.; Hanton, L. R.; Paul, R. L. *J. Chem. Soc., Chem. Commun.* **1992**, 235.
(46) (a) Moraczewski, J.; Geiger, W. E. *J. Am. Chem. Soc.* **1979**, *101*, 3407. (b) Grzeszczuk, M.; Smith, D. G.; Geiger, W. E. *J. Am. Chem. Soc.* **1983**, *105*, 1772.
(47) Representative Ni(III) structures: (a) van der Merwe, M. J.; Boeyens, J. C. A.; Hancock, R. D. *Inorg. Chem.* **1983**, *22*, 3489. (b) Wieghardt, K.; Walz, W.; Nuber, B.; Weiss, J.; Orzarowski, A.; Stratemeier, H.; Reinen, D. *Inorg. Chem.* **1986**, *25*, 1650. (c) Machida, R.; Kimura, E.; Kushi, Y. *Inorg. Chem.* **1986**, *25*, 3461. (d) Miyamae, H.; Yamauchi, K.; Yamashita, M. *J. Chem. Soc., Dalton Trans.* **1991**, 2921.

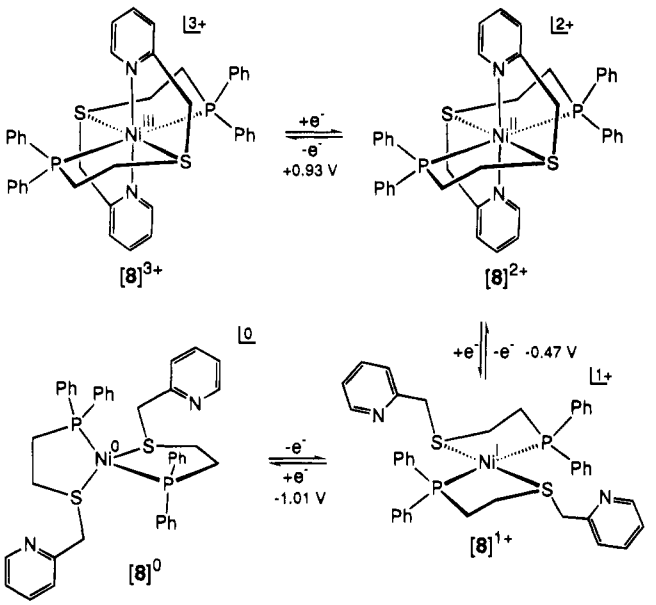

Figure 9. Electron transfer series based on $[Ni(pspyr)_2]^{2+}$, depicting established and proposed structures of complexes in four different oxidation states. Potentials refer to propylene carbonate solution and the SCE.

and a $...(d_{z^2})^1$ ground state. The Ni(III/II) reduction proceeds without change in coordination number. Electrochemical results for the Ni(II/I) couple, especially when compared to those for $[\mathbf{4}]^{2+/+}$, indicate a structural change; decoordination of the pendant pyridyl ligands to afford a four-coordinate Ni(I) species is consistent with the available results, but the structure of this species is not known. The structural systematics of Ni(I) are not extensively developed. Transitions between five-coordinate Ni(II/I)[43] and five-coordinate Ni(II)/four-coordinate Ni(I)[48] have been demonstrated; tetrahedral and planar structures are often stabilized (at least in part) by ligand steric demands,[16,18,48,49] especially for planar macrocyclic species.[48,49] The Ni(I/0) couple approaches reversible behavior in the manner of $[\mathbf{4}]^{+/0}$. Because all four-coordinate Ni(0) complexes are tetrahedral, it is assumed that $[\mathbf{8}]^0 = [Ni(pspyr)_2]$ will adopt this stereochemistry. If its Ni(I) precursor is six- or five-coordinate, slow electron transfer might be expected for this couple, an effect that has been observed previously in five- to four-coordinate transitions of Ni(I/0) couples of arsine[45] and phosphine[50] complexes. As with $[\mathbf{8}]^{+/0}$, reversible behavior is closely approached in strictly four-coordinate chelated Ni(I/0) couples with bis(diphosphine) ligation.[50]

Summary. The following are the principal results and conclusions of this investigation.

1. Complexes **6** and $[\mathbf{8}]^{2+}$ possess facially coordinated, hard–soft, tridentate ligands and pseudooctahedral complexes. In the absence of steric conflicts, the NiP_2S_2 planar units assume a cis configuration likely dictated by the trans influence of the tertiary phosphines.

2. Complex **6** can be oxidized to the Ni(III) species $[\mathbf{6}]^+$ with the same overall stereochemistry and a $...(d_{z^2})^1$ ground state; the complex cannot be reversibly reduced, presumably because of tight binding of axial anionic (carboxylate) ligands.

3. A four-membered electron transfer series based on $[\mathbf{8}]^{2+}$ can be generated by a combination of electrochemical and chemical reactions that are metal-centered and encompass the oxidation states Ni(0–III). In terms of coordination number, the following scheme (Figure 9) is consistent with all observations: Ni(III)(6) ⇄ Ni(II)(6) ⇄ Ni(I)(4) ⇄ Ni(0)(4). The structure of the Ni(I) species is least certain; four-coordinate nonplanar NiP_2S_2 stereochemistry is favored.

4. This work demonstrates that multiple oxidation states of nickel can be stabilized in a mixed hard–soft donor environment with neutral ligands capable of accommodating coordination numbers 4–6. The lack of ligand charge favors pyridyl decoordination upon reduction of Ni(II). Although the pspyr ligand is not a simulator of ligand binding in a protein, it does provide a demonstration that the physiological oxidation states of nickel, Ni(I,II,III), are unlikely to be traversed in any environment without accompanying alteration(s) in stereochemistry.

Last, we observe that a more extensive redox series than that in Figure 9 has been achieved by Downard *et al.*,[45] who were able to stabilize *five* oxidation states using chelating tertiary arsine ligands: Ni(IV)(6) ⇄ Ni(III)(5) ⇄ Ni(II)(5) ⇄ Ni(I)(5) ⇄ Ni(0)(4). Once again, the stereoelectronic preferences of nickel mandate structural changes within the series.

Acknowledgment. This research was supported by NSF Grant CHE 92-08387. X-ray diffraction equipment was obtained through NIH Grant 1 S10 RR 02247. We thank Professor W. H. Armstrong for use of a magnetic susceptibility balance and M. C. Muetterties and M. J. Scott for experimental assistance.

Supplementary Material Available: X-ray crystallographic results for the compounds in Table 1, including tables of positional and thermal parameters and interatomic distances and angles (11 pages). See any current masthead page for ordering information.

(48) Latos-Grażyński, L.; Olmstead, M. M.; Balch, A. L. *Inorg. Chem.* **1989**, *28*, 4065.

(49) (a) Furenlid, L. R.; Renner, M. W.; Szalda, D. J.; Fujita, E. *J. Am. Chem. Soc.* **1991**, *113*, 883. (b) Suh, M. P.; Kim, H. K.; Kim, M. J.; Oh, K. Y. *Inorg. Chem.* **1992**, *31*, 3620.

(50) Miedaner, A.; Haltiwanger, R. C.; DuBois, D. L. *Inorg. Chem.* **1991**, *30*, 417.